Theor Chim Acta (1995) 91: 333–351

Theoretica Chimica Acta

Ab initio study of the HCO_3^-/H_2O exchange in the $(NH_3)_3Zn^{II}(HCO_3^-)$ complex

Miquel Solà[1], José L. Andrés[1], Miquel Duran[1], Agustí Lledós[2], Juan Bertrán[2]

[1] Departament de Química, Universitat de Girona, Plaça de l'hospital 6, 17071 Girona, Catalonia, Spain

[2] Departament de Química, Universitat Autònoma de Barcelona, 08193 Bellaterra, Catalonia, Spain

Received August 15, 1994/Final revision received November 12, 1994/Accepted November 17, 1994

Summary. The displacement of bicarbonate anion in the $(NH_3)_3Zn^{II}(HCO_3^-)$ complex with water has been studied through *ab initio* calculations. It has been found that H_2O binds to the $(NH_3)_3Zn^{II}(HCO_3^-)$ species yielding a stable pentacoordinate $(NH_3)_3Zn^{II}(HCO_3^-)(H_2O)$ complex. The results also indicate that deprotonation of water in the pentacoordinate species facilitates the release of HCO_3^-, although, the presence of HCO_3^- in the coordination sphere of Zn^{II} makes such deprotonation more difficult. Environmental effects have been considered in the study of HCO_3^-/H_2O exchange.

Key words: Carbonic anhydrase (CA) – HCO_3^-/H_2O exchange – Continuum model – Environmental effects

Introduction

Carbonic anhydrase (CA) is a zinc metalloenzyme that catalyzes the reversible hydration of CO_2 to yield bicarbonate anion with an exceptional efficiency [1–7] X-ray data [5–11] show that the zinc atom placed at the active site of CA is bound to three imidazole groups coming from His94, His 96, and His119, whereas a water molecule completes a nearly symmetrical tetrahedral coordination geometry. In addition, the active site involves other proteinic residues along with eight ordered water molecules which are of functional importance.

It is almost universally accepted that a zinc-bound hydroxide ion is the nucleophile in this catalytic reaction [3–7, 12]. A simplified model for its mechanism involves the following four steps [4]: (1) proton transfer from Enzyme $Zn^{II}(OH_2)$ ($EZn^{II}(OH_2)$) in order to generate the catalytic species $EZn^{II}(OH^-)$; (2) binding of CO_2 near the active species $EZn^{II}(OH^-)$; (3) generation of the EZn^{II}-bound HCO_3^- species; and (4) binding of a water molecule and release of HCO_3^-. Different experimental studies [13–17] have established the first step to be rate-limiting at high buffer concentrations. Given that the maximal turnover of

---

A contribution from the "Grup de Química Quàntica de l'Institut d'Estudis Catalans"

Human Carbonic Anhydrase II (HCAII) is measured to be $10^6\ s^{-1}$, the energy barrier for the proton transfer involved in step 1 must be close to 10 kcal/mol [18].

Considering specially step 4, after formation of EZn^{II}-bound HCO_3^- complex, the HCO_3^- species is displaced by a water molecule and leaves the active site. This process has been barely studied, and can be formulated as

$$EZn^{II}(HCO_3^-) + H_2O \rightleftharpoons EZn^{II}(H_2O) + HCO_3^-. \qquad (1)$$

The nature of the bicarbonate intermediate has been widely investigated. Using Co(II), Mn(II), and Cu(II)-substituted CA, some authors [19] have found that the EZn^{II}-bound HCO_3^- complex is pentacoordinate, having the HCO_3^- ligand a bidentate coordination. Other studies [20] with Zn(II) complexes suggested that the HCO_3^- ligand is monodentate; therefore the Zn(II) dication having tetrahedral coordination. A very recent crystallographic analysis of the mutant Thr200- His Human Carbonic Anhydrase II performed at 1.9 Å resolution [21] shows the HCO_3^- ion bound in the active site to the Zn(II) as a pseudo-bidentate ligand. In this complex the metal has a coordination geometry between tetrahedral and trigonal bypiramide. Different experimental studies related to the HCO_3^-/H_2O exchange had been reported, the main question to be solved being whether a pentacoordinate $EZn^{II}(HCO_3^-)(H_2O)$ intermediate is formed during the exchange process. For instance [22], ESR spectra in a Co(II)-substituted CA revealed that a transient pentacoordinate intermediate exists, and that this complex might facilitate the exchange between bicarbonate and water ligands. Moreover, analysis of anionic inhibition in CA showed that during the exchange, a pentacoordinate metal transient intermediate is formed [7, 23]. A number of experimental work dealing with zinc pentacoordination [24–37] reinforces the possibility of its existence. Recently, four new works dealing with the possibility of pentacoordination in CA have emphasized the interest of this subject. First, the three-dimensional structure of a complex between catalytically active Co(II)-substituted Human CA-II and its substrate bicarbonate have been determined by X-ray crystallography [38]. Both bicarbonate and water ligands are coordinated. Second, in case of the mutant Thr200 → His, the affinity for bicarbonate is very much increased, then a crystal structure of this bicarbonated CA mutant has been obtained [21]. Nevertheless, the Zn water molecule has been displaced. Third, an X-ray structure of native HCA-II complexed with a formate anion has been reported [39a]. In this structure the Zn water molecule is still coordinated. Finally, the structure of the HCA-I-HCO_3^- complex reveals monodentate binding of the bicarbonate anion at apical tetrahedral position to the Zn ion [39b]. In conclusion, the posibility of Zn pentacoordinated complexes in HCO_3^-/H_2O exchange in CA is still open to further discussion.

As to theoretical studies, to our knowledge this exchange has been studied in three papers. In the first one, Liang and Lipscomb [40] showed that release of the HCO_3^- anion is facilitated by previous binding of water to Zn^{II}. In particular, their results gave that the energy barrier for the unfacilitated displacement of EZn^{II}-bound HCO_3^- with a water molecule is 169 kcal/mol, and that such a barrier is decreased to 109 kcal/mol when a fifth water ligand is considered. They also found that inclusion of some proteinic residues further reduces the energy barrier to 43 kcal/mol, and that deprotonation of this water ligand completely removes the energy barrier. In the second theoretical study, Merz et al. [18] used the AM1 semiempirical method to perform an exhaustive analysis of the different steps of the CA mechanism. These authors found that during the HCO_3^-/H_2O exchange, a pentacoordinate trigonal bipyramidal (tbp) complex is formed. In this complex, the water molecule occupies an equatorial position, whereas the bicarbonate anion is located at an axial site of the tbp. Furthermore, they showed that loss of the bicarbonate ion is aided by the presence of a number of water molecules. Finally, the authors proposed a new HCO_3^-/H_2O exchange mechanism implying an intramolecular proton transfer from the water ligand to the coordinated bicarbonate, prior to release of carbonic acid. However, this mechanism does not follow the experimental ping-pong kinetics; furthermore, carbonic acid has never been detected [41] either. Finally, Kraus and Garmer [42], using *ab initio* effective core potentials, found two stable pentacoordinate tbp structures. In these two complexes, the bicarbonate anion is located at an axial position. The first one has a water molecule located at an equatorial site and, the second one has a hydroxyl anion also located at an equatorial position. The removal of a proton from the water molecule of the $(NH_3)_3Zn^{II}(H_2O)(HCO_3^-)$ complex favours the release of bicarbonate anion by lowering its binding energy from 210 kcal/mol for this complex to the 105 kcal/mol for the $(NH_3)_3Zn^{II}(OH^-)(HCO_3^-)$ species. Then, these data reinforce the possibility that the first step would occur before the fourth. These authors also found that this effect is reinforced if the deprotonation of a coordinated histidine is also considered. Two more recent studies [43] by these two authors, analyse possible five-coordinated complexes involved in the catalytic mechanism.

From the aforementioned studies, one can see that several points concerning step 4 of the CA mechanism remain still unclear. First, it is difficult to understand how a strongly bound anion can be released and substituted by a neutral ligand like a water molecule. It is obvious that environmental effects will be of utmost importance in this exchange process. Second, it is also unclear whether a pentacoordinate or other intermediates complexes are formed during the HCO_3^-/H_2O exchange, and even if they do exist, their structure is unknown. Finally, the mechanism of this exchange process has not been definitively elucidated.

As a whole, the main goal of this article is to perform an *ab initio* study of the HCO_3^-/H_2O exchange using this exchange in the $(NH_3)_3Zn^{II}(HCO_3^-)$ species as a simplified model of the fourth step of the CA catalytic cycle. The specific purposes of the present work are the following: first, to study the possible existence of a pentacoordinate transient intermediate in the HCO_3^-/H_2O exchange; second, to analyse the structures and relative stabilities of all different pentacoordinate complexes that can be formed during this process; and third, to discuss all different possibilities suggested so far to explain the HCO_3^-/H_2O exchange in CA. Since the effect of the remainder proteinic residues and water molecules in the active site are deemed to be essential in the process, the environmental effect will also be taken into account.

Methodology

Ab initio all-electron SCF calculations were performed by means of the Hartree–Fock–Roothaan method [44]. Owing to computational limitations, three ammonia groups were used to simulate the three histidine ligands of the zinc ion. The validity of this substitution, which is necessary to limit the size of the chemical systems so that calculations be affordable, is supported by earlier studies of Kraus et al. [42] and Pullman et al. [45] who demonstrated that ammonia and imidazole transfer a similar amount of charge to Zn^{II}. The geometry of each NH_3 group was kept frozen, the N–H distances being 1.05 Å and the HNH angles being tetrahedral. Under these geometric constraints, full geometry optimizations were performed following Schlegel's method [46] or the Broyden–Fletcher–Goldfarb –Shanno (BFGS) [47–50] algorithm. The stationary points have established to be minima or transition states by numerical energy second derivatives in internal coordinates. Several authors [42, 51] pointed out that the structural information was shown to be reasonable calculated at this level of theory. For this reason, geometry optimizations were carried out with basis I. This basis set is a double ξ [52, 53] quality basis set for valence shells of all atoms, except for hydrogen atoms of the ammonia groups, for which the STO-3G basis set [54] was used. This basis set has been choosen because, at this level of theory, the ammonia and the imidazole group transfer a similar amount of charge to the Zn^{II}. Energies were recalculated with two different basis sets which included diffuse functions (basis II) and both diffuse and polarization functions (basis III). Basis II was basis I with an extra diffuse *sp* function [55] for O and C atoms of H_2O and HCO_3^- groups. Basis III was for Zn atom, a (14*s*, 11*p*, 6*d*)/[5*s*, 4*p*, 3*d*] contraction of Wachters [56] basis set for transition metals, including a 3*d* diffuse function following the Hay's series [57] with a 0.1539 exponent and, one term Gaussian fit to a STO 4f [58] as a polarization function with a 5.2 STO exponent [59]. For H_2O, OH^- and HCO_3^- groups, Basis III was also a double-ξ quality basis set for valence shells [60] with an *sp* diffuse function [55] and a *d* polarization function [61] for O and C atoms. For NH_3 groups, basis III was basis I with an extra *d* polarization function [61] for N atoms.

As it has been mentioned in the introduction, the environmental effect due to the rest of the protein has been taken into account. In the proteinic environment many differents effects influence the process. For instance, one can consider the presence of steric constraints, specific interactions like hydrogen bonds, electrostatic interactions due to the permanent charge distribution, polarization of the protein creating a reaction electric field, etc. In this work, we have only considered the polarization effect using the continuum model due to Tomasi et al. [62–64]. In this model the environment is represented by a continuous polarizable dielectric with permitivity ε and the solute is placed inside a cavity accurately defined by its own geometry [65]. Dielectric polarization due to the solute is simulated by the creation of a system of virtual charges on the cavity surface. The charge distribution on the surface polarizes in turn the charge distribution in the solute, this process being iterated until self-consistency in the solute electron density is achieved. In this way, the feedback effect of the environment on the solute is taken into account. The electrostatic contribution to the solvation free energy is found as the difference between the energies computed with the continuum model and without it less one-half the interaction energy between the charge distribution of the solute and the reaction field potential [63]. Moreover, the cavitation free energy is calculated with Pierotti's equation [66]. The optimized geometries in the gas phase ($\varepsilon = 1.00$) obtained with basis I were used throughout. Only recently, the analytical gradients for this continuum model of the environment have been reported, but the code for the optimization is not available yet [64b]. Theoretical studies of solvent effects [67, 68] on the tautomeric equilibrium of heterocycles have shown that molecular geometries change slightly with the relative permitivity of the medium. The main effect of the solvent reaction field is on the relative energies of the tautomers. Due to computational limitations, calculations which included environmental effects were carried out with basis I. In this work the study of surrounding medium effects has been performed using two different values of the dielectric constant, one corresponding to a n-hexane solution with a low dielectric constant ($\varepsilon = 1.88$), and the other corresponding to a water solution with a large dielectric constant ($\varepsilon = 78.36$). Given that reorientation of proteinic residues and water molecules at the active site is partially blocked, it seems that a low dielectric constant to model the environment should be used. However, a proteinic environment differs from a solvent, because in a protein there is a permanent electric field which has to be taken into account. Therefore, a continuum model like that used in this paper which was developed for solvents must be corrected in some way to account correctly for an enzymatic environmental effect. A large value of a dielectric constant will create a reaction field which accounts much better for the real electric field acting on the chemical system.

All calculations presented in this paper were carried out with the help of the GAUSSIAN 86 [69] and MONSTERGAUSS [70] programs. The surrounding medium effect was studied with a FORTRAN subroutine written by Tomasi and co-workers as incorporated in the MONSTERGAUSS program.

Results and discussion

Presentation of the results obtained is split into four sections. First, we analyse the thermodynamics of the HCO_3^-/H_2O global exchange; second, we study the different $(NH_3)_3Zn^{II}(HCO_3^-)(H_2O)$ pentacoordinate species and thermodynamics of the formation and dissociation processes; third, we discuss the formation mechanism of the five-coordinated systems; and fourth, we investigated the possible formation of the $(NH_3)_3Zn^{II}(HCO_3^-)(OH^-)$ species prior to HCO_3^- release.

Thermodynamics of the HCO_3^-/H_2O exchange

Once the $EZn^{II}(HCO_3^-)$ species has been formed, the next step in the CA catalytic cycle is the regeneration of the $EZn^{II}(H_2O)$ species. If one chooses the $(NH_3)_3Zn^{II}(H_2O)$ complex as a model for the CA active site, this process can be formulated as

$$(NH_3)_3Zn^{II}(HCO_3^-) + H_2O \rightleftharpoons (NH_3)_3Zn^{II}(H_2O) + HCO_3^-. \qquad (2)$$

For this reaction, the *in vacuo* energy gap between products and reactants at the SCF level is 205.4, 192.7 and 202.9 kcal/mol for basis I, II and III, respectively. Jacob et al. [71] reported earlier 184 kcal/mol for the same process using an extended basis set, whereas Liang and Lipscomb [40] found 169 kcal/mol with the PRDDO method. However, this energy gap is too large to account for the maximum experimentally allowed value of 10 kcal/mol in CA, previously mentioned. On this basis, it is not possible to understand how the HCO_3^- anion can be exchanged. Furthermore, inclusion of correlation energy at the MP2 level [72] (MP2/basis I//HF/basis I) does not change too much the result obtained at the SCF level, because it yields an energy gap of 205.3 kcal/mol, thus showing that the effect of correlation energy is not essential in this process. We must remark that this reaction can be regarded as a charge separation process where reactants having a global charge of + 1 form two products having global charges of + 2 and − 1. Therefore, surrounding medium effects should be especially important, being stabilized to a much larger extent the products than the reactants.

Environmental effects calculated with $\varepsilon = 1.88$ reduce the endothermicity of reaction (2) to 112.9 kcal/mol. This value is further decreased to 11.3 kcal/mol

Table 1. Solvation free energies (ΔG_{solv}) and their components (ΔG_{elec} and G_{cav}) for all stationary points found in the study of the HCO_3^-/H_2O exchange. All these values have been obtained with the basis set I, in two different environments of $\varepsilon = 1.88$ and 78.36. Energies are given in kcal/mol

	$\varepsilon = 1.88$			$\varepsilon = 78.36$		
	ΔG_{el}	G_{cav}	ΔG_{solv}	ΔG_{el}	G_{cav}	ΔG_{solv}
$(NH_3)_3Zn^{II}(HCO_3^-)$	− 33.2	11.3	− 21.9	− 73.4	18.8	− 54.6
$(NH_3)_3Zn^{II}(H_2O)$	− 91.9	10.1	− 81.8	− 195.6	16.7	− 178.9
$(NH_3)_3Zn^{II}(H_2O)_{eq}(HCO_3^-)_{ax}$ **weba**[a]	− 31.5	12.1	− 19.4	− 69.5	20.1	− 49.4
$(NH_3)_3Zn^{II}(H_2O)_{ax}(HCO_3^-)_{eq}$ **wabe**[a]	− 31.4	12.0	− 19.4	− 69.5	20.0	− 49.5
$(NH_3)_3Zn^{II}(H_2O)_{eq}(HCO_3^-)_{eq}$ **webe**[a]	− 32.1	11.9	− 20.2	− 71.6	19.8	− 51.8
$(NH_3)_3Zn^{II}(OH^-)_{eq}(HCO_3^-)_{eq}$ **hebe**[a]	− 11.3	11.6	0.3	− 28.1	19.4	− 8.7
H_2O	− 3.0	3.7	0.7	− 7.6	5.5	− 2.1
HCO_3^-	− 36.9	5.1	− 31.8	− 79.9	8.0	− 71.9

[a] w stands for water molecule, b for bicarbonate anion and *h* for hydroxyl anion. e stands for equatorial site and a for axial site in a tbp structure

when a dielectric constant of 78.36 is used. The latter value is close to that expected experimentally. These values have been obtained from the solvation free energies of the different species that intervene in reaction (2), which are collected in Table 1. The values of this table reveal that, as expected, the stabilizing effect of the surrounding medium is more important in the products, especially in the case of the doubly charged $(NH_3)_3Zn^{II}(H_2O)$ complex.

This preliminar thermodynamical study has confirmed that introduction of environmental effects, even with a simple continuum model, is essential to obtain results closer to experience.

$(NH_3)_3Zn^{II}(HCO_3^-)(H_2O)$ *species*

This section is structured as follows: first, the geometries of the optimized $(NH_3)_3Zn^{II}(HCO_3^-)(H_2O)$ complexes are reported; and second, relative energies of the zinc pentacoordinated complexes obtained and binding energies of HCO_3^- to the $(NH_3)_3Zn^{II}(H_2O)$ are examined.

Optimized geometries. The aim of this section is to explore the possible formation of a stable pentacoordinate complex when an incoming water molecule binds to the product $(NH_3)_3Zn^{II}(HCO_3^-)$. In this geometry optimization process, we have allowed the variables defining the coordination about the zinc atom to vary freely. This means that, starting from a given geometry, the optimized final complex may have any possible structure, e.g., trigonal bipyramidal (tbp), square pyramid (sp), an arrangement halfway between these two possibilities, or even a tetrahedral structure with loss of a ligand. Since a number of possible minima in the hypersurface exists, the final result will be very dependent on the geometry of the starting point and the optimization method employed. In order to examine the possible $(NH_3)_3Zn^{II}(HCO_3^-)(H_2O)$ pentacoordinate complexes, we have performed our geometrical optimizations starting from different points: first, the $(NH_3)_3Zn^{II}(HCO_3^-)_{ax}(H_2O)_{eq}$ complex (hereafter named **weba** because of the location of the water and bicarbonate ligands) reported earlier by other authors [18, 42]; second,

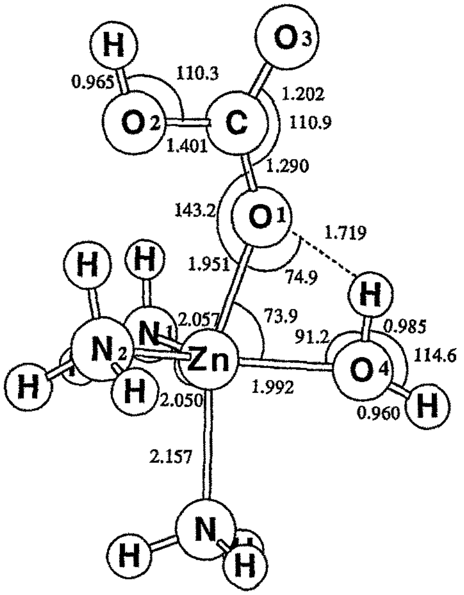

weba

Fig. 1. Optimized structure of $(NH_3)_3Zn^{II}(HCO_3^-)_{ax}(H_2O)_{eq}$ complex

the $(NH_3)_3Zn^{II}(HCO_3^-)_{eq}(H_2O)_{ax}$ complex (hereafter named **wabe**); third, the $(NH_3)_3Zn^{II}(HCO_3^-)_{eq}(H_2O)_{eq}$ complex (hereafter named **webe**); and, finally, the $(NH_3)_3Zn^{II}(HCO_3^-)_{ax}(H_2O)_{ax}$ complex (hereafter named **waba**).

Figure 1 shows the most important geometric parameters obtained in the optimization of complex **weba**. In this complex, water and bicarbonate are equatorial and axial ligands, respectively, giving rise to a quite distorted tbp arrangement. The value of the axial angle $N_{ax}\widehat{Zn}O_1$ is 158.4°, while those of the equatorial angles are 115.7° ($N_{eq1}\widehat{Zn}N_{eq2}$), 114.2° ($N_{eq2}\widehat{Zn}O_4$), and 129.4° ($O_4\widehat{Zn}N_{eq1}$). As rationalized earlier by Rossi and Hoffmann [73], the Zn–N axial bonds are longer than the equatorial ones. Interestingly, there is an intramolecular hydrogen bond between the O_1 atom and one of the hydrogens of water accounting, partially, for the distortion from the ideal tbp geometry.

The optimized geometrical parameters of complex **wabe** are given in Fig. 2. This complex also presents a quite distorted tbp geometry. In this pentacoordinate complex, the axial angle $N_{ax}\widehat{Zn}O_4$ is 166.3°, whereas the equatorial angles $N_{eq1}\widehat{Zn}N_{eq2}$, $N_{eq2}\widehat{Zn}O_1$, and $O_1\widehat{Zn}N_{eq1}$, are 119.1°, 114.9°, and 123.3°, respectively. Comparing with complex **weba** there is also an intramolecular hydrogen bond between the O_1 atom and one of the hydrogens of water, although the O_1–H bond length is now 0.1 Å longer. Thus, the O_1–H hydrogen bond in this complex is weaker than in complex **weba**. The Mayer bond orders [74] for these two hydrogen bonds, which are 0.091 and 0.072 for the complexes **weba** and **wabe**, respectively, reinforce this conclusion. As pointed out previously by Rossi and Hoffmann [73] for d^{10} ML_5 tbp complexes, an axial ligand transfers less charge to the central atom than an equatorial ligand does. For this reason, the bicarbonate ligand of complex **wabe** has transferred 0.018 electrons more than that of complex **weba** has. Therefore, O_1 of complex weba is more negative than O_1 of complex **wabe** (-0.886 vs. -0.876). Likewise, the hydrogen of water forming the intramolecular hydrogen

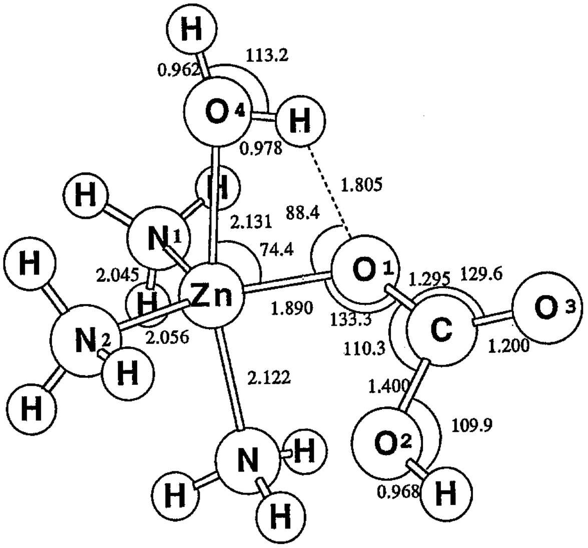

wabe

Fig. 2. Optimized structure of $(NH_3)_3Zn^{II}(HCO_3^-)_{eq}(H_2O)_{ax}$ complex

bond is more positive in complex **weba** than in complex **wabe** (0.504 vs. 0.483), thus explaining the stronger O_1–H hydrogen bond obtained for complex **weba**.

The most important geometrical parameters of complex **webe** are presented in Fig. 3. This complex has a quite regular tbp arrangement, with an axial angle $N_{ax1}\widehat{Zn}N_{ax2}$ of 179.6°, and equatorial angles of 118.7° $(O_4\widehat{Zn}O_1)$, 119.4° $(O_1\widehat{Zn}N_{eq})$, and 121.8° $(N_{eq}\widehat{Zn}O_4)$, which add up to 359.9°. No intramolecular hydrogen bond is detected in this structure.

Starting the optimization from complex $(NH_3)_3Zn^{II}(HCO_3^-)_{ax}(H_2O)_{ax}$, with bicarbonate and water as axial ligands, a free ammonia molecule is released, and the distorted tetrahedral $(NH_3)_2Zn^{II}(HCO_3^-)(H_2O)$ complex is formed. Therefore, a pentacoordinate complex having axial bicarbonate and water is not a minimum in the full potential energy hypersurface. As shown earlier by Rossi and Hoffmann [73], strong σ-donors stabilize a tbp when located in equatorial sites. In contrast, this geometry is unfavoured when σ-donors are placed in axial sites. Therefore, the presence of bicarbonate and water in axial positions explains the breaking of the initial tbp geometry. In spite of this fact, complex **weba** with bicarbonate in an axial site of the tbp is a minimum because of the strong intramolecular hydrogen bond formed which stabilizes the tbp structure. The pentacoordinated structure with a water molecule found by Kraus and Garmer [42] was similar to this **weba** complex and also presented a hydrogen bond which stabilized the tbp structure.

Interestingly, the $Zn–O_1$ Mayer bond order changes from 0.584 in the tetrahedral complex $(NH_3)_3Zn^{II}(HCO_3^-)$ to 0.392, 0.455, and 0.500 in the pentacoordinate complexes **weba, wabe**, and **webe**, respectively. Therefore, the binding of a water molecule as a fifth ligand increases the $Zn–O_1$ distance (which is 1.844 Å in the $(NH_3)_3Zn^{II}(HCO_3^-)$ complex) and reduces the bicarbonate bond strength, as pointed out previously by some authors [35, 45, 75]. This fact is especially remarkable in complex **weba**, where the bicarbonate ligand occupies an axial site of the tbp

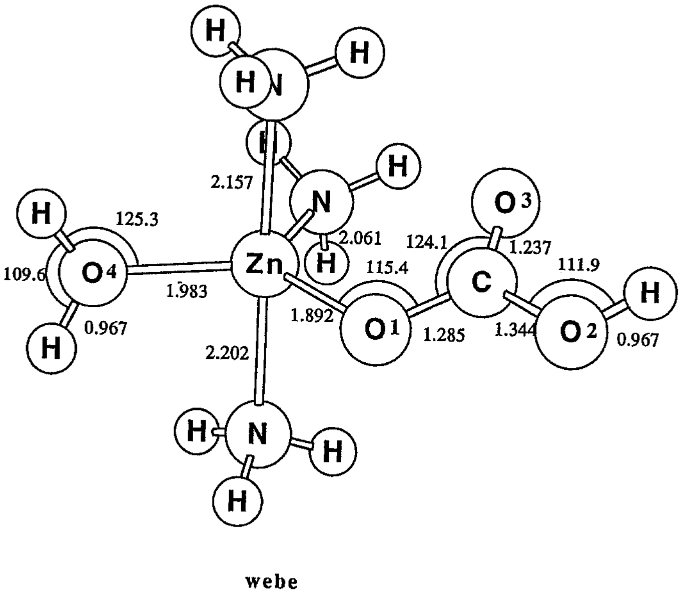

Fig. 3. Optimized structure of $(NH_3)_3Zn^{II}(HCO_3^-)_{eq}(H_2O)_{eq}$ complex

because, as it is well known, for d^{10} ML_5 tbp complexes σ-donors form stronger bonds when they are located in equatorial positions [73].

Energetics. Three different pentacoordinate complexes with water and bicarbonate ligands in the coordination sphere of Zn^{II} have been found as stable species. All these pentacoordinate Zn^{II} species found in our study feature a trigonal bipyramidal arrangement. Previous theoretical calculations reported the same result for similar Zn^{II} complexes [18, 42, 75a, 76] An indication of their stabilities can be gained from the binding energies of a water molecule to the $(NH_3)_3Zn^{II}(HCO_3^-)$ complex. These energies, which correspond to reaction (3), are gathered in Tables 2 and 3:

$$(NH_3)_3Zn^{II}(HCO_3^-) + H_2O \rightleftharpoons (NH_3)_3Zn^{II}(HCO_3^-)(H_2O). \qquad (3)$$

In Table 2, one can see the well-known overestimation of the binding energy when it is computed with small basis sets (basis I). While the water binding energy for **webe** is corrected when basis II (basis I plus diffuse functions) is used, for **weba** and **wabe** complexes the main change is obtained when polarization functions are also included (basis III). It can be due to the intramolecular hydrogen bond that **weba** and **wabe** complexes present. To estimate the hydrogen bond energy between HCO_3^- anion and H_2O molecule, the formation energy of the $HCO_3^- \cdot H_2O$ cluster was computed with basis I–III. These hydrogen bond energies were 20.7, 18.5 and 12.9 kcal/mol for basis I, II and III, respectively. One can see that the strength of the hydrogen bond is largely overestimated when polarization functions are not included. Our best results give **webe** and **wabe** species as the most stable ones. It agrees with the fact that strong σ-donors in d^{10} ML_5 complexes prefer equatorial positions of the tbp [73]. In spite of the improvement of the basis sets being correlated with a decrease in the water binding energy, these energies are still

Table 2. Binding energies (in kcal/mol) of a water molecule to the $(NH_3)_3Zn^{II}(HCO_3^-)$ complex, for three different basis sets

	Basis I	Basis II	Basis III
weba	– 26.5	– 21.4	– 6.4
wabe	– 26.4	– 20.9	– 10.4
webe	– 22.3	– 14.2	– 13.1

Table 3. Binding energies (in kcal/mol) of a water molecule to the $(NH_3)_3Zn^{II}(HCO_3^-)$ complex, for three different values of the dielectric constant

	$\varepsilon = 1.00$	$\varepsilon = 1.88$	$\varepsilon = 78.36$
weba	– 26.5	– 24.8	– 19.2
wabe	– 26.4	– 24.7	– 19.2
webe	– 22.3	– 21.4	– 17.4

important to assure the existence of the pentacoordinate complexes. This is specially valid for the **webe** structure.

In Table 3, the water binding energies for three different values of dielectric constants are presented. As found previously [75a], the water binding energy decreases by the environmental effect due to the smaller charge transfer from ligands to the Zn atom. This lowering is more important for **weba** and **wabe** complexes because they have an intramolecular hydrogen bond. In a polar medium, the energy of such bonds decreases. From all these results, complex **webe** emerges as the most probably intermediate in the HCO_3^-/H_2O interconversion process.

Now, we consider the thermodynamics for the dissociation of the five-coordinated species. Tables 4 and 5 assemble the dissociation energy of the different pentacoordinate $(NH_3)_3Zn^{II}(HCO_3^-)(H_2O)$ species into the HCO_3^- anion and $(NH_3)_3Zn^{II}(H_2O)$ for both three different basis sets and three different dielectric constants of the surrounding medium. This process corresponds to

$$(NH_3)_3Zn^{II}(HCO_3^-)(H_2O) \rightleftharpoons (NH_3)_3Zn^{II}(H_2O) + HCO_3^- . \tag{4}$$

The dissociation energies of the pentacoordinate $(NH_3)_3Zn^{II}(HCO_3^-)(H_2O)$ species in the HCO_3^- anion and $(NH_3)_3Zn^{II}(H_2O)$ collected in Table 4 reveal the intrinsic difficulty to release this anion. This dissociation energy decreases when the basis sets are augmented, but it is still too high. A dissociation energy for **weba** complex into HCO_3^- and $(NH_3)_3Zn^{II}(H_2O)$ of 209.3 kcal/mol agrees very well with the value found by Kraus et al. (210.0 kcal/mol) [42]. The most appealing aspect of the energies shown in Table 5 is the important reduction of the dissociation energy of the pentacoordinate species into HCO_3^- and $(NH_3)_3Zn^{II}(H_2O)$ upon the increase of the dielectric constant value. This point can be easily interpreted from the values of Table 1 which collects the solvation free energies (ΔG_{solv}) and their components (ΔG_{el} and G_{cav}) for all the stationary points found in the study of step (4) of CA mechanism. As mentioned above, the final products of HCO_3^- release, which are $(NH_3)_3Zn^{II}(H_2O)$ and HCO_3^-, have the larger ΔG_{solv}. Therefore, they are

Table 4. Dissociation energies of the optimized $(NH_3)_3Zn^{II}(HCO_3^-)$ (H_2O) complexes into HCO_3^- and $(NH_3)_3Zn^{II}(H_2O)$ (in kcal/mol) for the three different basis sets

	Basis I	Basis II	Basis III
weba	231.9	214.1	209.3
wabe	231.8	213.5	213.3
webe	227.7	206.6	216.1

Table 5. Dissociation energies of the optimized $(NH_3)_3Zn^{II}(HCO_3^-)$ (H_2O) complexes into HCO_3^- and $(NH_3)_3Zn^{II}(H_2O)$ (in kcal/mol) for the three different values of the dielectric constant

	$\varepsilon = 1.00$	$\varepsilon = 1.88$	$\varepsilon = 78.36$
weba	231.9	137.7	30.5
wabe	231.8	137.6	30.5
webe	227.7	134.3	28.7

the species which stabilized most owing to the surrounding medium, thus explaining the important decrease of the HCO_3^- binding energy which facilitates the release of HCO_3^-. Thus, as suggested earlier [18, 35, 71] medium effects become essential to understand the HCO_3^- release in CA mechanism. Nonetheless, the dissociation energies of the pentacoordinated complexes in $(NH_3)_3Zn^{II}(H_2O)$ and HCO_3^- in a medium of $\varepsilon = 78.36$ are still too large to account for experimental data.

Formation mechanism of the pentacoordinated species.

The main discussion of the pentacoordinated species formation is to know the relative stability of the five-coordinated complexes with respect to the four-coordinated ones (forming the first shell) with a H_2O molecule in a second shell. The second-shell H_2O molecule can form hydrogen bonds either to the NH_3 or HCO_3^- groups. We only present here complexes which have the H_2O molecule bonded with the HCO_3^- anion. Complexes with the H_2O making hydrogen bonds with the ammonia groups are meaningless because ammonia is used as a model of the imidazol group present in the proteinic residue. Fig. 4a, b show complexes formed when a H_2O molecule in the second shell interacts with the $(NH_3)_3Zn^{II}(HCO_3^-)$ complex. These two structures have been characterized as a minima on the potential energy surface by numerical second derivatives in internal coordinates. Figure 4a shows a complex which will give the **wabe** structure (hereafter named **pro-wabe**) and Fig. 4b shows a complex which will give **weba** species (hereafter named **pro-weba**). The **wabe** and **pro-weba** complexes show a bidentate bicarbonate ligand. Previous studies [75b, c] at the same level of theory show a monodentate bicarbonate ligand when the second shell water molecule was not considered, then the bidentate character of the HCO_3^- anion can be due to the presence of the second-shell H_2O molecule. Isoelectron density contour maps of

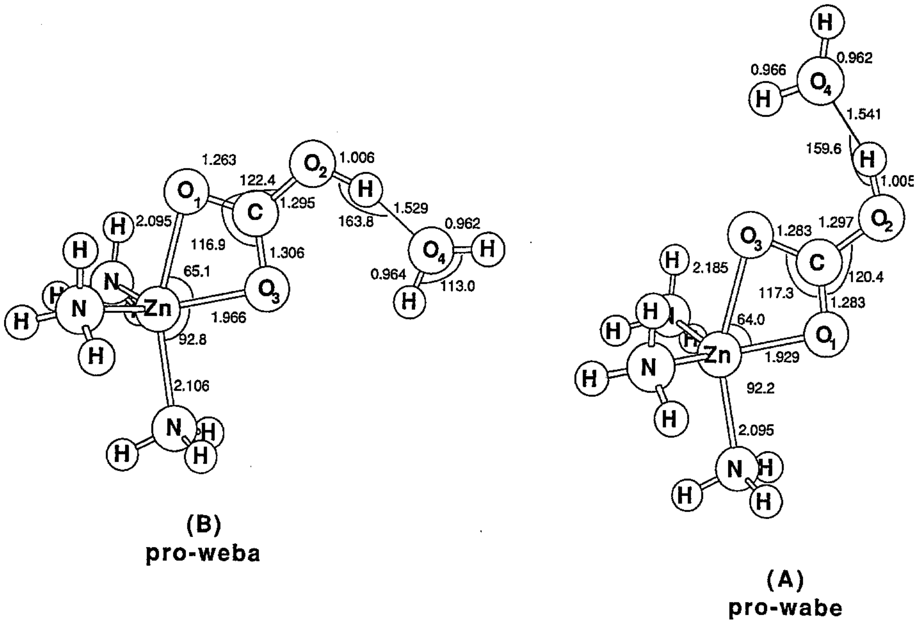

Fig. 4. Optimized structure of $(NH_3)_3Zn^{II}(HCO_3^-)(H_2O)_{2ndshell}$ complexes

Table 6. Energies of the intermediates **pro-wabe** and **pro-weba** (in kcal/mol) with respect to the optimized pentacoordinate **wabe** and **weba** complexes, respectively, for three different values of the dielectric constant

	$\varepsilon = 1.00$	$\varepsilon = 1.88$	$\varepsilon = 78.36$
pro-wabe	0.1	1.3	−2.1
pro-weba	0.3	1.2	0.1

the **pro-wabe** and **pro-weba** structures confirm this conclusion showing a ring critical point between $Zn–O_1–C–O_3$ atoms [77]. A related of complexes with bidentate ligands have also been found experimentally using X-ray diffraction by Liljas et al. [21]. However, although protons are not observable, the X-ray structure have been interpreted to indicate that a hydroxyl is bound to Zn. This X-ray interpretation clearly differs from geometries presented in Fig. 4. In Table 6, the relative energies of **pro-wabe** and **pro-weba** intermediates with respect to the **wabe** and **weba** complexes for the three dielectric constants are given. Both **pro-weba** and **pro-wabe** species have almost the same energy as the **weba** and **wabe** final complexes, even when the environment has been taken into account.

Figure 5 shows the transition state for formation the **wabe** complex. This transition state shows migration of the H_2O molecule from second shell to the first shell. In this transition state one of the $Zn–O_3$ bond of bicarbonate has been broken and the $Zn–O_4$ bond is being formed, in such a way that from transition state geometry, this mechanism can be described as being dissociative–associative. The energy barrier of this process is 4.5 kcal/mol for formation of **wabe** species.

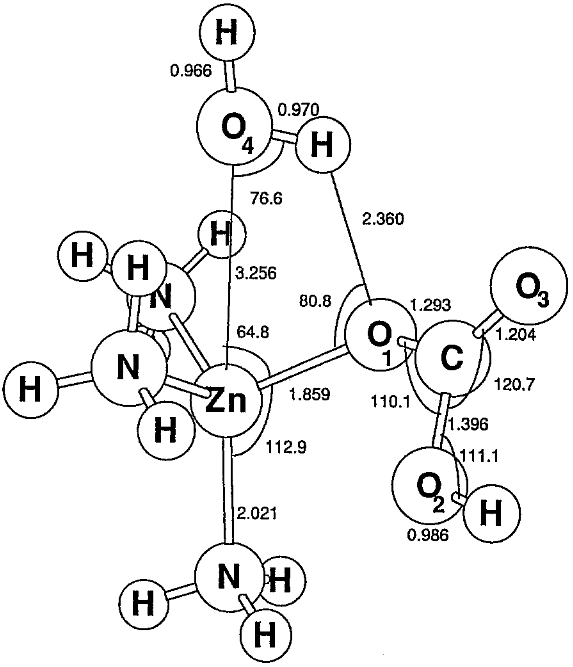

Fig. 5. Optimized structure of the transition state of the formation of the wabe pentacoordinated complex

This barriers is small and lesser than 10 kcal/mol, for this reason, formation of the five-coordinated species does not seem to be the limitant step of the whole HCO_3^-/H_2O exchange process. The low energetic barrier of this transition state supports the formation of the pentacoordinated species in the HCO_3^-/H_2O exchange mechanism. In consequence, the possibility of a dissociative mechanism in which the HCO_3^- is released prior to the formation of the $(NH_3)_3Zn^{II}(H_2O)$ complex has not been considered because the dissociation of the HCO_3^- from $(NH_3)_3Zn^{II}(HCO_3^-)$ should have a larger barrier due to the dissociation in the bicarbonate anion and the $(NH_3)_3Zn^{II}$ cation.

$(NH_3)_3Zn^{II}(HCO_3^-)(OH^-)$ *species*

Once water binds to the $(NH_3)_3Zn^{II}(HCO_3^-)$ species, there are different alternatives to regenerate the $(NH_3)_3Zn^{II}(OH^-)$ active species. The first one, is the direct release of HCO_3^- to yield first the $(NH_3)_3Zn^{II}(H_2O)$ complex, and then the $(NH_3)_3Zn^{II}(OH^-)$ complex through an intramolecular proton transfer to His64. The deprotonation is carried out first, through a two-water bridge [13] from $EZn(H_2O)$ to His64, and in a second step from this group to the buffer. As shown in a previous section (Tables 4 and 5) this process is unlikely due to the high energetic cost even in a surrounding medium of $\varepsilon = 78.36$. Another possibility suggested first by Pullman [45b] and studied more recently by Merz et al. [18] with the AM1 method, concerns the intramolecular proton transfer from water to HCO_3^- to yield the $(NH_3)_3Zn^{II}(H_2CO_3)(OH^-)$ species, where release of H_2CO_3 would be very easy. Any attempt made to optimize this complex has given negative results, as we have always obtained complexes **weba** or **wabe**. Kraus and Garmen [42] have found similar results. Therefore, one can conclude that complex

$(NH_3)_3Zn^{II}(H_2CO_3)(OH^-)$ is not a true minimum on the potential energy hypersurface, and thus is not a stable species. Besides, from an experimental point of view, H_2CO_3 has never been detected [41] during the CO_2/HCO_3^- interconversion. Finally, another alternative suggested first by Liang and Lipscomb [40] deals with a previous deprotonation of water to give the $(NH_3)_3Zn^{II}(HCO_3^-)(OH^-)$ species before the release of HCO_3^-. In this complex the posterior loss of the bicarbonate anion will be easier because Zn^{II} complexes with two anions in the coordination sphere are quite unstable [75a, 78]. Further, release of HCO_3^- would directly furnish the $(NH_3)_3Zn^{II}(OH^-)$ catalytic active species. In this section all possible $(NH_3)_3Zn^{II}(HCO_3^-)(OH^-)$ complexes are analysed.

Optimized geometries. All coordination possibilities about the zinc atom in complex $(NH_3)_3Zn^{II}(HCO_3^-)(OH^-)$ have been studied. Only the pentacoordinate complex with both the hydroxyl and the bicarbonate anions occupying axial sites has been initially disregarded from the outcome of our previous study [75a] showing the unstability of the tbp d^{10} ML_5 complexes with two anions located in axial positions. Therefore, we have started optimizations from complex $(NH_3)_3Zn^{II}(HCO_3^-)_{ax}(OH^-)_{eq}$ (hereafter named **heba** for the positions of hydroxyl and bicarbonate anions in the coordination sphere), complex $(NH_3)_3Zn^{II}(HCO_3^-)_{eq}(OH^-)_{ax}$ (hereafter named **habe**), and complex $(NH_3)_3Zn^{II}(HCO_3^-)_{eq}(OH^-)_{eq}$ (hereafter named **hebe**). It has been noticed that complexes **heba** and **habe** lose an ammonia ligand during the optimization process to yield the $(NH_3)_2Zn^{II}(HCO_3^-)(OH^-)$ tetrahedral complex, showing that the Zn^{II} ion at the active site cannot accommodate two negative charges in its inner sphere [78] On the contrary, complex **hebe**, with hydroxyl and bicarbonate ligands occupying equatorial positions, is indeed a stable complex. The stability of this comlex can be easily interpreted from the Rossi and Hoffmann hypothesis [73] on the preferences of σ-donors for equatorial sites in the tbp d^{10} ML_5 complexes.

Figure 6 shows the geometry of complex **hebe**, which has an almost regular tbp structure. The axial angle $N_{ax}\widehat{Zn}N_{ax}$ is 169.3°, and the sum of the equatorial angles, of 102.7° ($N_{eq}\widehat{Zn}O_1$), 135.5° ($O_1\widehat{Zn}O_4$), and 121.9° ($O_4\widehat{Zn}N_{eq}$) is 360.1°. The presence of the two anions in equatorial sites results in a large $O_1\widehat{Zn}O_4$ angle. The Zn–O_1 and Zn–O_4 bond lengths, together with their Mayer bond orders (0.399 and 0.748, respectively), indicate that the hydroxyl anion binds more strongly to Zn^{II} than bicarbonate does. This result has been already obtained experimentally by Kimura et al [33, 34] in a model for CA.

Energetics. From an energetic point of view there are two features worth being remarked. First, as previously emphasized [75a, 78],Zn^{II} pentacoordinate complexes with two anions in the coordination sphere are quite unstable, so formation of the $(NH_3)_3Zn^{II}(HCO_3^-)(OH^-)$ complex will facilitate the release of HCO_3^-. Second, it is well known that binding of an anion originates an important increase in the deprotonation energies of the ligands in a complex [32–34, 75a, 79], so deprotonation of water in the $(NH_3)_3Zn^{II}(HCO_3^-)(H_2O)$ complexes will be more difficult than in the $(NH_3)_3Zn^{II}(H_2O)$ species. In this section these two energetic aspects are analysed.

The dissociation energies of HCO_3^- in complex **hebe** are 131.8, 114.4 and 125.7 kcal/mol for basis sets I, II and III, respectively. A HCO_3^- dissociation energy of 105 kcal/mol for a pentacoordinate complex with hydroxyl anion has been reported by Kraus et al. [42]. However, this reported complex has the HCO_3^- in an axial site, which corresponds to an **heba** structure. Given that the axial ligands are less strongly bounded than the equatorial ones, this discrepancy is not surprising.

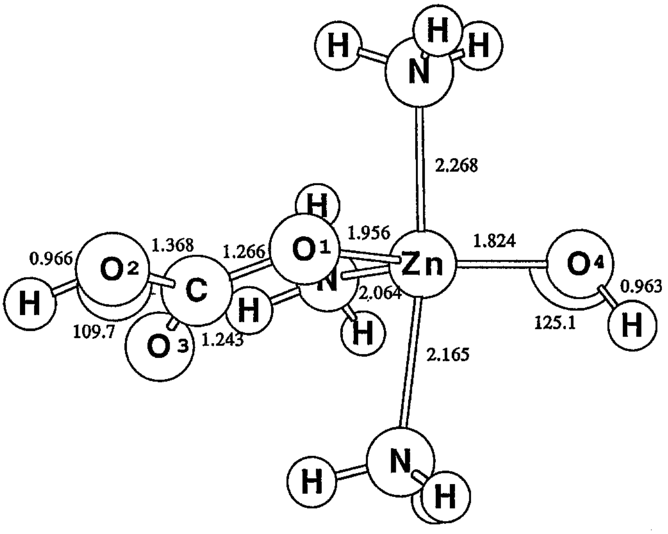

hebe

Fig. 6. Optimized structure of $(NH_3)_3Zn^{II}(HCO_3^-)_{eq}(OH_-)_{eq}$ complex

Despite the HCO_3^- dissociation energy change for the different basis sets, this energy is always so big that this process will not take place in a medium of $\varepsilon = 1.00$. The most important decrease in the HCO_3^- dissociation energy is due to the environment. The dissociation energy of HCO_3^- anion in complex **hebe** (131.8 kcal/mol in vacuum, $\varepsilon = 1.00$) is reduced to 76.6 and 16.0 kcal/mol in surrounding media of $\varepsilon = 1.88$, and $\varepsilon = 78.36$, respectively. These values can be compared with those given in Table 5 for the $(NH_3)_3Zn^{II}(HCO_3^-)(H_2O)$ complexes. One can see that in the gas phase the energy required to extract HCO_3^- from complex **hebe** is 100.1 kcal/mol lower than from complex **weba**. Therefore, deprotonation of water facilitates the HCO_3^- release. This difference decreases with the increase of the dielectric constant. In particular, in a surrounding medium of $\varepsilon = 78.36$ this discrepancy is only 14.5 kcal/mol. In this latter case, loss of the bicarbonate anion in complex **hebe** costs only 16.0 kcal/mol, which is closer to that expected from experimental data.

In Tables 7 and 8 the deprotonation energies (DPE) for reaction (5) are presented for both three different basis sets and three different dielectric constants.

$$(NH_3)_3Zn^{II}(HCO_3^-)(H_2O) + H_2O \rightarrow (NH_3)_3Zn^{II}(HCO_3^-)(OH^-) + H_3O^+ \quad (5)$$

Despite the change in the DPE in the gas phase with the basis sets, the deprotonation process of the tetracoordinate complex (reaction 6) has a minor energetic cost than the deprotonation of the pentacoordinate ones. However, when

$$(NH_3)_3Zn^{II}(H_2O) + H_2O \rightarrow (NH_3)_3Zn^{II}(OH^-) + H_3O^+ \quad (6)$$

a medium of $\varepsilon = 78.36$ is considered, the DPE of the tetracoordinate complex, following reaction (6), is raised to 40.3 kcal/mol, and the DPE of the, for instance, complex weba decreases to 51.0 kcal/mol. In the gas phase, the difference between the DPE of the tetracoordinate complex and that of, for instance, complex **weba**,

Table 7. Water deprotonation energies (in kcal/mol) for pentacoordinate **weba, wabe**, and **webe** complexes, for three different basis sets

	Basis I	Basis II	Basis III
weba	84.5	84.9	79.3
wabe	84.2	84.3	83.3
webe	80.3	77.7	86.0

Table 8. Water deprotonation energies (in kcal/mol) for pentacoordinate **weba, wabe,** and **webe** complexes in the gas phase and in surrounding media of $\varepsilon = 1.88$ and $\varepsilon = 78.36$

	$\varepsilon = 1.00$	$\varepsilon = 1.88$	$\varepsilon = 78.36$
weba	84.5	68.7	51.0
wabe	84.2	68.6	51.0
webe	80.3	65.3	49.2

is greater than 80 kcal/mol. However, in a surrounding medium of $\varepsilon = 78.36$, the difference in the DPEs decreases to merely 10.7 kcal/mol. Therefore, it can be concluded that, in a surrounding medium of large dielectric constant, presence of a bicarbonate anion in the coordination sphere does not change very much the deprotonation energy of water.

It is worth noting that there are two factors which counteract. On the one hand, deprotonation of water facilitates the release of HCO_3^-; on the other hand, presence of HCO_3^- in the coordination sphere makes deprotonation of water difficult. The importance of both factors is reduced with the increase in the dielectric constant. Notwithstanding, our results suggest that prior to bicarbonate release, it might be a deprotonation of the coordinated water in order to generate the $(NH_3)_3Zn^{II}(HCO_3^-)(OH^-)$ species. Two recent theoretical studies have found a similar result using a model for the description of the active site of the CA close to the model used in this work [40, 42].

Conclusions

In this paper the existence of stable pentacoordinate complexes in the HCO_3^-/H_2O exchange process in the $(NH_3)_3Zn^{II}(HCO_3^-)$ complex has been analysed. Three different pentacoordinate tbp complexes with water and bicarbonate ligands in the coordination sphere of Zn^{II} have been found. The binding energies are overestimated with small basis sets, like basis I. However, the water binding energy with large basis sets, like basis III, is still big enough to assure the existence of a pentacoordinate complex as **webe**. Therefore, the possibility that the mechanism of the HCO_3^-/H_2O exchange in CA could go through a pentacoordinated complex is reinforced. This point needs to be clarified with new experimental studies. The path to obtain the pentacoordinated complexes is the migration of a water molecule from the solvation second-shell to the first-shell. Either **pro-wabe** and **pro-weba** complexes or **wabe** or **weba** species have essentially the same energy then, the energetic cost for the dissociation of bicarbonate will be very similar in any case. In the pentacoordinated complexes (**wabe**, **weba** and **webe**), direct release of the HCO_3^- anion is energetically difficult, even when surrounding medium effects are taken into account. This has led to examine two other feasible mechanisms of HCO_3^-/H_2O exchange.

In the first mechanism, it has been concluded that complex $(NH_3)_3Zn^{II}(H_2CO_3)(OH^-)$, obtained by means of an intramolecular proton transfer from water to bicarbonate, is not a true minimum in the potential energy hypersurface. From these results and from experimental data, the possibility of release of H_2CO_3 instead of release of HCO_3^- has been rejected.

The alternative of proton transfer before release of HCO_3^- has been also pondered. It has been found that complex $(NH_3)_3Zn^{II}(HCO_3^-)(OH^-)$ is stable only when two anionic ligands occupy equatorial positions in the tbp. From an energetic point of view there are two factors which counterbalance: first, deprotonation of water facilitates the HCO_3^- release; second, presence of HCO_3^- anion makes more difficult deprotonation of water. From these two factors that counteract, it emerges that the difficulty in the deprotonation of water is compensated by the ease of bicarbonate release. Our results show that considering the effect of the surrounding medium is essential in order to get a realistic description of the process. The alternative process in which the OH^- anion binds to the $(NH_3)_3Zn^{II}(HCO_3^-)$ has been disregarded due to the high energetic cost of the desolvation energy of an OH^- anion.

Our simplified model for the description of the active site and the proteinic environment in CA, and the limitations of the level of calculations do not allow us to obtain a definitive answer to the mechanism of HCO_3^-/H_2O exchange in the CA. Nevertheless, the question of a previous or simultaneous deprotonation of the Zn-bounded water molecule with respect to the bicarbonate release must not be disregarded.

Acknowledgment. We acknowledge Dr. A. Liljas for supplying preprints prior to publication.

References

1. Prince RH, Woolley PR (1972) J Chem Soc Dalton Trans 1548
2. Williams TJ, Henkens RW (1985) Biochemistry 24:2459
3. Sen AC Tu, CK Thomas H, Wvnns GC, Silverman DN (1986) In: Bertini I, Luchinat C, Maret W, Zeppezauer M. (eds) Zinc enzymes, Vol I. Birkhäuser, Boston, p. 329
4. Silverman DN, Lindskog S (1988) Acc Chem Res 21:30
5. Woolley P (1975) Nature 258:677
6. Bertini I, Luchinat C (1983) Acc Chem Res 16:272
7. Pocker Y, Deits TL (1982) J Am Chem Soc 104:2424
8. Kannan KK, Petef M, Fridborg K, Lövgren S, Ohlsson A, Petef M (1975) Proc Natl Acad Sci USA 72:51
9. Kannan KK, Petef M, Fridborg K, Cid-Dresdner H, Lövgren S (1977) FEBS Lett 73:115
10. Liljas A, Kannan KK, Bergsten P-C, Waara I, Fridborg K, Strandberg B, Carlbom U, Järup L, Lövgren S, Petef M (1972) Nature New Biol 235:131
11. Eriksson EA, Jones TA, Liljas A (1986) In: Bertini I, Luchinat C, Maret W, Zeppezauer M (eds) Zinc enzymes Vol I. Birkhäuser, Boston, p. 317
12. Davis RP (1959) J Am Chem Soc 81:5674
13. Pocker Y, Janjić N (1989) J Am Chem Soc 111:731
14. Silverman DN, Tu CK (1975) J Am Chem Soc 97:2263

15. Coates JH, Gentle GJ, Lincoln SF (1974) Nature 249:773
16. Pocker Y, Miao CH (1987) Biochemistry 26:8481
17. Steiner H, Jonsson B-H, Lindskog S (1975) Eur J Biochem 59:253
18. Merz Jr, KM, Hoffmann R, Dewar MJS (1989) J Am Chem Soc 111:5636
19. (a) Bertini I, Canti G, Luchinat C, Mani F (1981) J Am Chem Soc 103:7784; (b) Led JJ, Neesgaard E (1987) Biochemistry 26:183; (c) Haffner PH, Coleman JE (1975) J Biol Chem 250:996
20. (a) Looney A, Han R, McNeil K, Parkin G (1993) J. Am Chem Soc 115:4690; (b) Williams TJ, Henkens RW (1985) Biochemistry 24:2459; (c) Darensbourg DJ, Meckfessel Jones ML, Reibenspies JH (1993) Inorg Chem 32:4675
21. Xue Y, Vidgren J, Svensson LA, Liljas A, Jonsson B-H, Lind-skog S (1993) Proteins 15:80
22. Haffner PH, Coleman JE (1975) J Biol Chem 250:996
23. Moratal JM, Martínez-Ferrer M-J, Donaire A, Castells J, Salgado J, Jiménez HR (1991) J Chem Soc Dalton Trans 3393
24. Nakacho Y, Misawa T, Fujiwara T, Wakawars A, Tomita K (1976) Bull Chem Soc Jpn 49:595
25. (a) Grewe H, Udupa MR, Krebs B (1982) Inorg Chim Acta 63:119; (b) Kai Y, Morita M, Yasuoka N, Kasai N (1985) Bull Chem Soc Jpn 58:1631; (c) Takahashi K, Nishida Y, Kida S (1984) Bull Chem Soc Jpn 57:2628; (d) Bencini A, Bianchi A, Garcia-España E, Mangani S, Micheloni M, Orioli P, Paoletti P (1988) Inorg Chem 27:1104
26. Monzingo AF, Matthews BW (1984) Biochemistry 23:5724
27. Kato M, Ito T (1985) Inorg Chem 24:509
28. Harrison PG, Begley MJ, Kikabhai T, Killer F (1986) J Chem Soc Dalton Trans 929
29. Lebioda L, Stec B (1989) J Am Chem Soc 111:8511
30. Holmes MA, Matthews BW (1981) Biochemistry 20:6912
31. Kuo LC, Makinen MW (1982) J Biol Chem 257:24
32. Kimura E, Koike T, Toriumi K (1988) Inorg Chem 27:3687
33. Kimura E, Shiota T, Koike T, Shiro M, Kodama M (1990) J Am Chem Soc 112:5805
34. Kimura E, Koike T (1991) Comments Inorg Chem 11:285
35. Auf der Heyde TPE, Nassimbeni LR (1984) Acta Crystallographica B40:582
36. Zhang C, Chadha R, Reddy HK, Schrauzer GN (1991) Inorg Chem 30:3865
37. Kirchner C, Krebs B (1987) Inorg Chem 26:3569
38. Hakansson K, Wehnert A (1992) J Mol Biol 228:1212
39. (a) Hakansson K, Carlsson M, Svensson LA, Liljas A (1992) J Mol Biol 227: 1192; (b) Kumar V, Kannan KK (1994) J. Mol. Biol. 241:226
40. (a) Liang J-Y, Lipscomb WN (1989) Int J Quantum Chem 36:299; (b) Liang J-Y, Lipscomb WN (1989) Int J Quantum Chem 36:299
41. Khalifah RG (1980) In: Bayer C, Gros G, Bartels H (eds) Biophysics and physiology of carbon dioxide. Springer, New York, p 206
42. Kraus M, Garner DR (1991) J Am Chem Soc 113:6426
43. (a) Garmer DR, Kraus M (1992) J Am Chem Soc 114:6487; (b) Garmer DR, Kraus M (1992) Int J Quantum Chem 42:1469
44. Roothaan CCJ (1951) Rev Mod Phys 23:69
45. (a) Demoulin D, Pullman A (1978) Theoret Chim Acta 49:161; (b) Pullman A (1981) Ann N Y Acad Sci 367:340
46. Schlegel HB (1982) J Comp Chem 3:214
47. Broyden CG (1970) Math Comp 24:365
48. Fletcher R (1970) Comput J 13:317
49. Goldfarb D (1970) Math Comp 24:23
50. Shanno DF (1970) Math Comp 24:647
51. Kitchen DB, Allen LC (1989) J Phys Chem 93:7265
52. Binkley JS, Pople JA, Hehre WJ (1980) J Am Chem Soc 102:939
53. Dobbs KD, Hehre WJ (1987) J Comp Chem 8:861
54. Hehre WJ, Stewart RF, Pople JA (1969) J Chem Phys 51:2657
55. Clark T, Chandrasekhar J, Spitznagel GW, Schleyer P von R (1983) J Comp Chem 4:294
56. Wachters AJH (1970) J Chem Phys 52:1033
57. Hay PJ (1977) J Chem Phys 66:4377
58. Stewart RF (1970) J Chem Phys 52:431

59. Rosi M, Baushchlicher CW (1989) J Chem Phys 90:7264
60. Hehre WJ, Ditchfield R, Pople JA (1972) J Chem Phys 56:2257
61. Hariharan PC, Pople JA (1973) Theoret Chim Acta 28:213
62. Miertuš S, Scrocco E, Tomasi J (1981) Chem Phys 55:117
63. Pascual-Ahuir JL, Silla E, Tomasi J, Bonaccorsi R (1987) J Comp Chem 8:778
64. (a) Floris F, Tomasi J (1989) J Comp Chem 10:616; (b) Cammi R, Tomasi J (1994) J Chem Phys 100:7495
65. The sphere radii used for atoms were 20% larger than the van der Waals (or ionic) radii, (hydrogen, 1.44 Å; Å; carbon, 1.94 Å; nitrogen, 1.80 Å; oxygen, 1.68 Å; zinc, 0.84 Å). The surrounding medium effect calculations were carried out at 298.15 K
66. Pierotti RA (1976) Chem Rev 76:717
67. Karelson MM, Katritzky AR, Szafran M, Zerner MC (1989) J Org Chem 54:6030
68. Karelson MM, Katritzky AR, Szafran M, Zerner MC (1990) J Chem Soc Perkin Trans. 2:195
69. Frisch MJ, Binkley JS, Schlegel HB, Raghavachari K, Melius, CF, Martin RL, Stewart JJP, Bobrowicz FW, Rohlfing CM, Kahn LR, Defrees DF, Seeger R, Whiteside RA, Fox DJ, Fleider EM, Pople JA (1984) Program GAUSSIAN86, Carnegie-Mellon Quantum Chemistry Publishing Unit, Pittsburgh PA
70. Peterson MR, Poirier RA (1981) Program MONSTERGAUSS, Department of Chemistry, University of Toronto, Ontario, Canada
71. Jacob O, Cardenas R, Tapia O (1990) J Am Chem Soc 112:8692
72. Møller C, Plesset MS (1934) Phys Rev 46:618
73. Rossi AR, Hoffmann R (1975) Inorg Chem 14:365
74. Mayer I (1986) Int J Quantum Chem 29:477
75. (a) Solà M, Lledós A, Duran M, Bertrán J (1991) Inorg Chem 30:2523; (b) Solà M, Lledós A, Duran M, Bertrán J (1992) J Am Chem Soc 114:869; (c) Solà M, Lledós A, Duran M, Bertrán J (1992) In: Bertrán J (ed) Molecular aspects of biotechnology: computational models and theories; Kluwer Academic Press, The Netherlands, p 263
76. Giessner-Prettre C, Jacob O (1989) J Comput-Aided Mol Design 3:23
77. Bader RWF (1985) Acc Chem Res 18:9
78. Pocker Y, Deits TL (1981) J Am Chem Soc 103:3949
79. Bertini I, Luchinat C, Rosi M, Sgamellotti A, Tarantelli F (1990) Inorg Chem 29:1460